

# LASER SEEDING SCHEMES FOR SOFT X-RAYS AT LCLS-II

G. Penn, LBNL, Berkeley, CA, USA

P. Emma, E. Hemsing, G. Marcus, T.O. Raubenheimer, L. Wang, SLAC, Menlo Park, CA, USA

## Abstract

The initial design for LCLS-II incorporates both SASE and self-seeded configurations. Increased stability and/or coherence than is possible with either configuration may be provided by seeding with external lasers followed by one or more stages of harmonic generation, especially in the soft x-ray regime. External seeding also allows for increased flexibility, for example the ability to quickly vary the pulse duration. Studies of schemes based on high-gain harmonic generation and echo-enabled harmonic generation are presented, including realistic electron distributions based on tracking through the injector and linac.

## INTRODUCTION

In addition to SASE [1] and self-seeding [2, 3] schemes, LCLS-II [4] may also incorporate seeding using external lasers. Benefits include more control over the x-ray pulse, better shot-to-shot stability, and possibly a narrower spectrum. The use of external lasers may have an impact on repetition rate and tends to reduce the energy of the final x-ray pulse. In addition, upshifting by very large harmonics from the laser wavelength introduces new challenges. Here we discuss designs for both the two-stage high-gain harmonic generation (HG) and single-stage echo-enabled harmonic generation (EEHG) seeding schemes, and compare their performance. Two-stage HG with a fresh-bunch delay has been demonstrated at FERMI@Elettra [5] with excellent performance down to the 65th harmonic (4 nm). EEHG has been demonstrated at NLCTA [6] up to the 15th harmonic (160 nm).

## ELECTRON BEAM AND UNDULATOR PARAMETERS

The simulations shown below use particles obtained from two start-to-end (S2E) simulations of the linac accelerating the beam to 4 GeV. One simulation uses a 100 pC bunch and the other a 300 pC bunch. Not all aspects of longitudinal dynamics have been modelled, however. The nominal parameters for the electron beam and the main undulator sections for producing radiation are given in Table 1. Local parameters will vary with position along the bunch. The longitudinal phase space of the beams are shown in Fig. 1, and the current profiles are shown in Fig. 2. Compared to the 100 pC bunch, the 300 pC bunch is longer, has a larger emittance and a slightly lower peak current.

The final undulators have a period of 39 mm and cover the desired tuning range from 250 eV to 1.3 keV. Here, we focus on producing radiation at 1 nm, which is the most challenging part of the tuning range. The external laser is

fixed at a wavelength of 260 nm. The large overall harmonic jump presents certain challenges which will be noted below.

Table 1: Beam and Undulator Parameters for Soft X-ray Production at LCLS-II

Parameter	Symbol	Value
<b>Electron Beam:</b>		
Bunch charge	$Q$	100 — 300 pC
Electron energy	$E$	4 GeV
Peak current	$I$	1 kA
Emittance	$\epsilon_N$	0.3 — 0.43 $\mu\text{m}$
Energy spread	$\sigma_E$	0.5 MeV
Beta function	$\beta$	15 m
<b>Final undulators:</b>		
Undulator period	$\lambda_u$	39 mm
Undulator segment length	$L_{\text{seg}}$	3.4 m
Break length	$L_b$	1.2 m
Min. magnetic gap	$g_{\text{min}}$	7.2 mm
Max. undulator parameter	$K_{\text{max}}$	5.48
Max. resonant wavelength	$\lambda_{\text{max}}$	5.1 nm

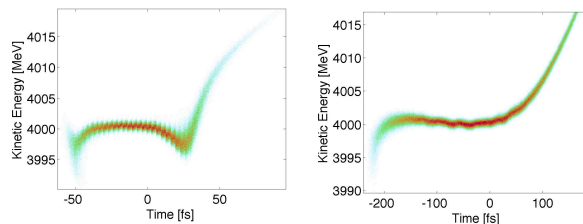


Figure 1: Longitudinal phase space for 100 pC (left) and 300 pC (right) electron bunches.

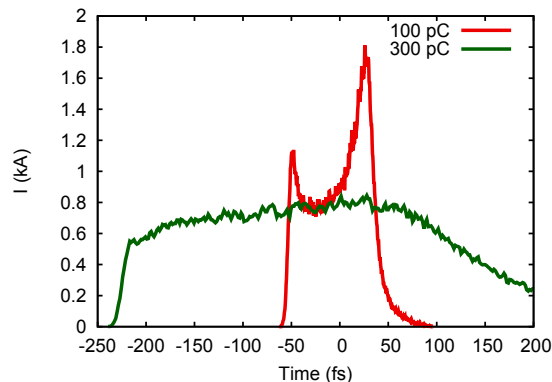


Figure 2: Current profiles for 100 pC and 300 pC electron bunches.

## HGHG AND EEHG SCHEMES

The layouts for the two main schemes are shown in Fig. 3. Additional undulator sections may be placed at the end, tuned to a shorter wavelength. FEL simulations were performed using GENESIS [7]. These and other schemes have previously been considered in Chapter 18 of the LCLS-II Conceptual Design Report [8] for idealized beams and with a focus on producing radiation at 2 nm.

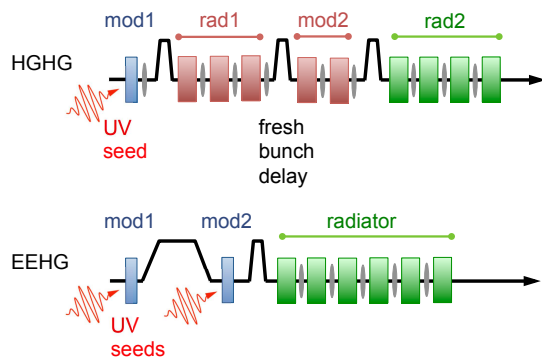


Figure 3: Beamline layouts using EEHG (top) and two-stage HGHG with a fresh bunch delay (bottom).

### HGHG Design and Layout

The initial HGHG design uses one laser with a 260 nm wavelength. One stage of harmonic generation is followed by a fresh-bunch delay and a second stage of harmonic generation to reach wavelengths as low as 1 nm. The nominal peak power to reach 1 nm is 800 MW, but the laser power has to be adjusted differently for the two beams because radiation production at the intermediate wavelength is sensitive to the electron properties. Because of the fresh-bunch delay the pulse duration must be short in order to have the two stages fit within the core of the electron bunch.

The undulator used for the initial modulation has a period of 100 mm and is 3.2 m long. The resulting energy modulation can be as large as 6 MeV. The next five undulator sections have a period of 80 mm, each 3.2 m long. These undulators have helical polarization to increase the coupling at the intermediate wavelength; all other undulators have planar polarization. The first three are used to radiate through the narrow bunching produced at a 260 nm wavelength. This is followed by a delay chicane, and the next two undulator sections modulate electrons in a region which is located further to the head of the bunch. The large total undulator length is required to be able to reach a final wavelength of 1 nm. The intermediate wavelength in that case is 13 nm, the 20th harmonic.

The third chicane yields bunching at 1 nm of the order of 1%. The final set of undulators, with a 39 mm period, radiate at this wavelength to saturation. The final stage of harmonic generation must produce significant bunching at the 13th harmonic, so the energy modulation must be quite large as well, but at the same time radiation at 1 nm will be

suppressed if the energy spread grows beyond around 3 MeV. Note that both bunches have a minimum energy spread of 0.5 MeV.

The chicanes are fairly modest, and are all about 2 m in length. The first chicane has  $R_{56} = 22 \mu\text{m}$ . The fresh-bunch delay can be as small as 25 fs, corresponding to  $R_{56} = 15 \mu\text{m}$ , in order to fit the entire process into the 100 pC bunch length. For the 300 pC bunch, the delay could be as large as 100 fs. The weaker end of this range for the delay chicane is not enough to suppress bunching at the intermediate wavelength. The bunching towards the tail of the bunch will radiate in the undulator sections immediately following the fresh bunch delay, although not enough to produce significant bunching after next stage of harmonic generation.

### EEHG Design and Layout

Echo-enabled harmonic generation (EEHG) [9] operates through a form of wave-mixing, where two energy modulations are used instead of one for standard HGHG. The first modulation is followed by a chicane which strongly over-bunches the modulation, creating well-separated bands in longitudinal phase space. Each band has a reduced energy spread. The second modulation is also followed by a chicane but in this case they are tuned so as to perform a standard phase rotation of each band. The overall bunching factor can be significant even at very high harmonics.

For the EEHG example, we consider two seed lasers both with a wavelength of 260 nm. The first undulator section is 3.2 m long, with a period of 0.1 m, identical to the first undulator used for HGHG. The laser pulse going into this undulator has a peak power of 47 MW, and generates an energy modulation of 1.5 MeV. This is followed by a chicane with  $R_{56} = 14.37 \text{ mm}$ . The second undulator is also 3.2 m long but with a period of 0.4 m. The laser pulse going into this undulator has a peak power of 900 MW, and generates an energy modulation of 2 MeV. Both lasers have a Rayleigh length of 1 m. The pulse duration can be anywhere from 10s to 100s of fs. This is followed by a chicane with  $R_{56} = 53 \mu\text{m}$ . Bunching is generated directly at 1 nm.

The reason for the difference in undulator periods is that in the second undulator the phase space bands in the beam are particularly sensitive to energy scattering. Increasing the period lowers the magnetic field and reduces incoherent synchrotron radiation (ISR). For the same reason, the large dispersion required for the first chicane is obtained by increasing the length of the magnets rather than increasing the magnetic field. Thus, the first chicane is 9 m long with 2 m dipole magnets, while the second chicane is only 2 m long. Even without magnetic fields, there is intra-beam scattering (IBS) which pushes the design towards being as short as possible. The combined effect of both ISR and IBS reduces the bunching factor at 1 nm from an ideal value of 5.2% to roughly 1.4%. Without taking into effect the impact of scattering, the optimal bunching parameter would be given

by the magnitude of

$$\hat{b} = \sum_{\substack{m,p \\ k_X = k_2 p - k_1 m}} e^{i(p\psi_2 - m\psi_1)} (-1)^p \quad (1)$$

$$\times J_p(C_2 \eta_{m2}) J_m(C_1 \eta_{m1}) e^{-iC_1 \bar{\eta}} e^{-C_1^2 \sigma_{\bar{\eta}}^2 / 2},$$

where  $C_1 = k_X R_2 - k_1 m R_1$ ,  $C_2 = k_X R_2$ ,  $\psi_{1,2}$  are the laser phases,  $k_{1,2}$  are the laser wavenumbers, and  $k_X$  is the target output wavenumber. The relative energy spread  $\sigma_{\eta} = \sigma_E/E$ , the relative height of the two energy modulations are  $\eta_{m1}$  and  $\eta_{m2}$ , and  $\bar{\eta}$  is the local relative energy offset. Usually only one term in the summation contributes significantly to the bunching, and this term is generally selected to correspond to  $m = 1$ . Note that normally  $|C_1| \ll |C_2|$ , which results in reduced sensitivity to both energy spread and energy chirps.

After the bunching is generated, the electron beam goes directly into undulator sections with a 39 mm undulator period. Radiation is produced at 1 nm and amplified to saturation.

## SIMULATION RESULTS

We show results for producing radiation at 1 nm. Shorter wavelengths and higher harmonics are in general more challenging. Performance improves dramatically for longer wavelengths, but 1 nm (1.2 keV) has been selected because it is the upper end of the tuning range for soft x-rays at LCLS-II.

For two-stage HGHG, we present results when going from a 260 nm external laser to a 13 nm intermediate wavelength to 1 nm. The final x-ray properties are shown in Fig. 4 for both 100 pC and 300 pC bunches. The output pulse energy at 1 nm is 7  $\mu$ J for the 100 pC bunch and 4  $\mu$ J for the 300 pC bunch. There are several major differences in the parameter settings for these examples. The 100 pC bunch offers a very short interval in which to perform each stage of harmonic generation, thus the fresh-bunch delay is set to only 25 fs. Even with a short pulse duration, the external laser tends to blow up the energy spread in the second half of the bunch. Therefore, a super-Gaussian distribution is used with power  $\propto \exp(-t^4/t_0^4)$  having a fwhm duration of 20 fs. For the 300 pC bunch, the fresh bunch delay can be increased to 100 fs, and the external laser is a regular Gaussian with 40 fs fwhm. Because the 300 pC bunch has larger transverse emittances and suffers from more longitudinal variations than the 100 pC bunch, the peak power must be increased to 900 MW to compensate.

In both examples, short pulses are generated, although the 300 pC case shows significant SASE background occurring in those regions where the energy spread has not been increased. If the beamline were made longer, the total pulse energy would increase but the contrast becomes significantly worse. Figure 5 shows step-by-step profiles of the radiation at different wavelengths in the various stages of the FEL. The importance of slippage and the motivation for using a super-Gaussian external laser can be clearly seen in this example.

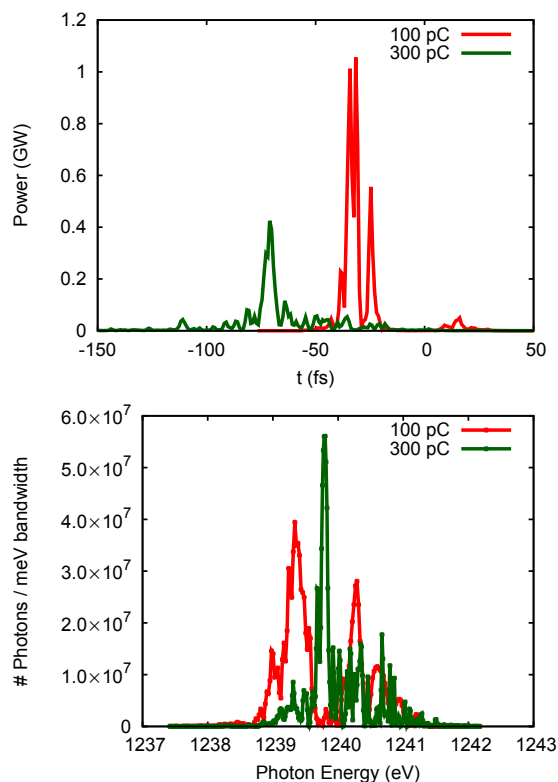


Figure 4: Power and spectral profiles of the final x-ray pulses for HGHG.

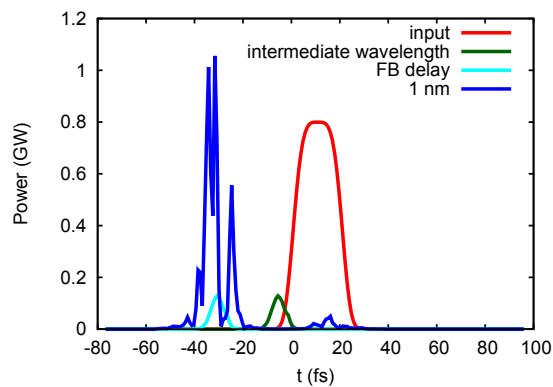


Figure 5: Power profile of the radiation at various stages in the HGHG beamline, for a 100 pC electron bunch.

The spectrum is quite broad in both cases, many times more than the transform limit. This is partially due to SASE background. More importantly, the large harmonic jump makes the beamline highly sensitive to any longitudinal variations in the electron beam. The performance improves greatly at wavelengths 2 nm or longer.

For EEHG going from a 260 nm external laser directly to 1 nm, the final x-ray properties are shown in Fig. 6 for both 100 pC and 300 pC bunches. Here, the configuration was not changed at all except for the external lasers, which have a 100 fs fwhm duration for the 100 pC bunch and a 200 fs fwhm duration for the 300 pC bunch, in order to take

advantage of the longer bunch length. For the 100 pC bunch the output pulse energy at 1 nm is 18  $\mu$ J with a 22 fs fwhm duration. The fwhm bandwidth is 0.13 eV, which is about 1.5 times the bandwidth limit. For the 300 pC bunch the output pulse energy at 1 nm is 25  $\mu$ J with a 45 fs fwhm duration. The fwhm bandwidth is 0.07 eV, which is also less than a factor of 2 from the transform limit. In both cases, the ratio of the duration of the output pulse to that of the second seed laser is roughly  $1.4(\lambda_2/\lambda_X)^{1/3}$ .

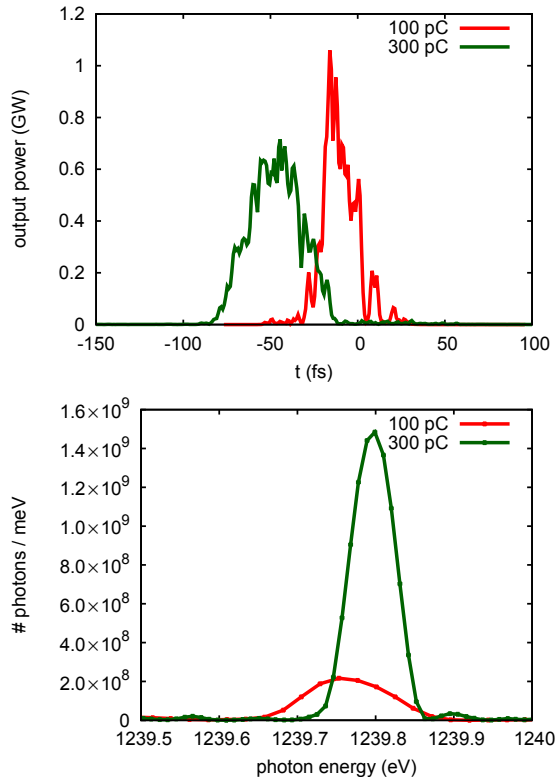


Figure 6: Power and spectral profiles of the final x-ray pulses for EEHG.

## CONCLUSION

The main limitation of the HGHG scheme is that the current bunch profile barely has enough length to support a fresh-bunch delay. However, pulses with several fs duration can be produced even for the 100 pC bunch. Longer bunches should allow for longer pulses. Further study is needed to determine what minimum bandwidth can be achieved; at 1 nm it may be only a modest reduction compared to SASE.

The EEHG seeding scheme should produce long pulses with good coherence, assuming that the second seed laser can be tightly controlled. The parameter settings, especially the chicane strengths, must be carefully set but are not depend much on the electron bunch properties. Not only small variations in beam quality but even large changes, such as in the bunch charge, should be able to be accommodated without re-adjustment. However, commissioning may be challenging, especially to reach 1 nm.

ISBN 978-3-95450-133-5

In both the two-stage HGHG and single-stage EEHG schemes, the energy spread is increased to above 2 MeV. The minimum energy spread generated in the seeded portion of the beam grows as the target wavelength is reduced. At the same time, the FEL bandwidth decreases. This increases the required undulator length to reach saturation, and reduces the final peak power. Competition with SASE from unseeded portions of the bunch also becomes a concern.

For the EEHG scheme, 1 nm seems to be approaching the limit for using EEHG. The two-stage HGHG scheme with a fresh bunch delay more sensitive to pre-existing energy chirps and energy modulations than the EEHG scheme. Therefore, for HGHG 1 nm may be at or even past the limit for producing pulses with stable temporal structure shot-to-shot. If stable or narrow spectral structure is required as well, that limit may be closer to 2 nm.

## ACKNOWLEDGMENT

This work was supported by the Director, Office of Science, Office of Basic Energy Sciences, of the U.S. Department of Energy under Contract Nos. DE-AC02-05CH11231 and DE-AC02-76SF00515.

## REFERENCES

- [1] R. Bonifacio, L. De Salvo, P. Pierini, N. Piovella, and C. Pellegrini. Spectrum, temporal structure, and fluctuations in a high-gain free-electron laser starting from noise. *Phys. Rev. Lett.*, 73:70–73, 1994.
- [2] J. Feldhaus, E.L. Saldin, J.R. Schneider, E.A. Schmeidmiller, and M.V. Yurkov. Possible application of x-ray optical elements for reducing the spectral bandwidth of an x-ray SASE FEL. *Optics Commun.*, 140:341–352, 1997.
- [3] G. Geloni, V. Kocharyan, and E. Saldin. A novel self-seeding scheme for hard x-ray FELs. *Journal of Modern Optics*, 58:1391–1403, 2011.
- [4] G. Marcus et al. FEL simulation and performance studies for LCLS-II. In *These Proceedings: Proc. 36th Int. Free Electron Laser Conf. JACoW, Basel, Switzerland, 2014*. TUP032.
- [5] E. Allaria, R. Appio, L. Badano, W.A. Barletta, S. Bassanese, S.G. Biedron, A. Borgia, E. Busetto, D. Castronovo, P. Cinquegrana, et al. Highly coherent and stable pulses from the fermi seeded free-electron laser in the extreme ultraviolet. *Nature Photonics*, 6:699–704, 2012.
- [6] E. Hemsing, M. Dunning, C. Hast, T.O. Raubenheimer, S. Weathersby, and D. Xiang. Highly coherent vacuum ultraviolet radiation at the 15th harmonic with echo-enabled harmonic generation technique. *Phys. Rev. ST Accel. Beams*, 17:070702, 2014.
- [7] S. Reiche. GENESIS 1.3: a fully 3D time-dependent FEL simulation code. *Nucl. Instr. Meth. A*, 429:243–248, 1999.
- [8] LCLS-II Design Study Group. LCLS-II conceptual design report. Report LCLSII-1.1-DR-0001-R0, SLAC, January 2014.
- [9] G. Stupakov. Using the beam-echo effect for generation of short-wavelength radiation. *Phys. Rev. Lett.*, 102:074801, 2009.